

---

# Metamorphic Marvel: Unraveling Lamprey Sex Dynamics and Ecosystem Implications

## Summary

Delving into the intricate dynamics of lamprey populations, we focus on their adaptive response to environmental conditions through alterations in sex ratios. Our study primarily consists of two parts: methodology and experiments.

We establish three distinct models, namely the **Population Dynamics (P.D.) Model**, **Mating Model (M. Model)**, and **Food Web Model (F.W. Model)** to form our **Large Lamprey Model (LLM)**. Each of these models corresponds to different time scales.

The **M. Model**, operating on a small time scale, scrutinizes the influence of mating behavior on the population. It incorporates pre-copulatory sexual selection, employing a **fitness variance-based** approach to gauge the strength of sexual selection. We utilize two **Bayesian Models** to explore the impact of individual phenotypic characteristics on lamprey mating dynamics.

Moving to a medium time scale, the **F.W. Model** explores the effects of multiple hosts and parasites on the population. Through the incorporation of a functional response function, the model describes how individual species acquire resources or engage in predation. The solution to the corresponding **Ordinary Differential Equations (ODE)** involves the use of the **Proper orthogonal decomposition (POD)** method for linear approximation, **Jacobi Diagonalization** for system decoupling, and the **Crank-Nicolson** method for numerical solution.

The **P.D. Model**, addressing a large time scale, studies the impact of dynamic growth on the population over decades. Building upon the Naive Model, this iteration incorporates the influence of the mating system, and the system is solved analytically to discern long-term population dynamics.

To fortify the credibility of the study, we select three representative lamprey species for experimental analysis and conduct a comparative study of two **Bayesian Models**.

For task 1, we compare sex ratio changes and stability across three indicators, namely the **Ecosystem Functionality**, the **Ecosystem Empowerment**, and the **Ecosystem Integrity**. We conclude from these three dimension that changing sex ratios enhances the performance of the larger ecological system.

For task 2, we predict lamprey populations at medium and large scales. Results indicating that the advantage of altering the sex ratio is to **expand populations in challenging environments**. However, it also points to the disadvantage of **significant population fluctuations** over time, leading to relatively poor stability.

For task 3, we make the simulation of the **P.W. model** 500 times. We notice that the group where the sex ratio is subject to alteration exhibits **greater variance** in the deviation of the **P.W. model**, indicating it will pose a **negative impact** on the stability of the ecosystem.

Finally, we predict changes in the populations of hosts and lamprey competitors for task 4, finding that altering the sex ratio provides **other parasites with an advantage** in the short term.

**Keywords:** Bayesian Model   Ordinary Differential Equations   Proper Orthogonal Decomposition  
Jacobi Diagonalization   Crank-Nicolson

# Contents

<b>1</b>	<b>Introduction</b>	<b>3</b>
1.1	Background . . . . .	3
1.2	Problem Restatement . . . . .	3
1.3	Our Work . . . . .	3
<b>2</b>	<b>Assumptions and Justifications</b>	<b>4</b>
<b>3</b>	<b>Notations</b>	<b>5</b>
<b>4</b>	<b>Methodology</b>	<b>5</b>
4.1	Large Lamprey Model (LLM) . . . . .	6
4.2	Population Dynamics (P.D. Model) . . . . .	6
4.2.1	Population Dynamics without Sex Variation . . . . .	6
4.2.2	Population Dynamics with Sex Variation . . . . .	6
4.3	Mating Model (M. Model) . . . . .	7
4.3.1	Birth Rate Resulting from Mating System . . . . .	7
4.3.2	First Bayesian Model Based on Sexual Selection . . . . .	8
4.3.3	Second Bayesian Model based on Identified Traits . . . . .	9
4.4	Modified Population Dynamic Model Considering the Mating System . . . . .	10
4.4.1	Setup of the Dual Logistic Model . . . . .	10
4.4.2	Solution to the Dual Logistic Model . . . . .	10
4.5	Food Web Model (F.W. Model) . . . . .	10
4.5.1	Single Species Functional Response . . . . .	11
4.5.2	Multispecies Functional Response . . . . .	11
4.5.3	Numerical Approaches to Solve the Response ODEs . . . . .	12
4.6	Model Evaluation . . . . .	14
<b>5</b>	<b>Numerical Results</b>	<b>15</b>
5.1	Preparation . . . . .	15
5.1.1	Case study: Setup of Three Representative Specimens . . . . .	15
5.1.2	Comparative Study: Comparison of two Bayesian Mating Models . . . . .	16
5.1.3	Parameter Choice and Numerical Simulation . . . . .	17
5.2	Responses to the Questions . . . . .	18
5.2.1	Impact on the Larger Ecological System Given Sex Alteration . . . . .	18
5.2.2	Advantages and Disadvantages of Sex Alteration on Lamprey Population . . . . .	19
5.2.3	Impact on the Stability of Ecological System Given Sex Alteration . . . . .	20
5.2.4	Impact on the Others in the Ecosystem . . . . .	22
<b>6</b>	<b>Sensitivity Analysis</b>	<b>22</b>
<b>7</b>	<b>Further Discussion</b>	<b>23</b>
7.1	Strengths . . . . .	23
7.2	Weaknesses . . . . .	24
<b>8</b>	<b>Conclusion</b>	<b>24</b>
<b>9</b>	<b>References</b>	<b>25</b>

# 1 Introduction

## 1.1 Background

Sea lampreys, characterized by a long, eel-like body and a round, jawless mouth filled with numerous rows of sharp teeth, play intricate roles in ecosystems. They are seen as parasites in some lake habitats while serving as a food source in some regions of the world as well. The sex determination in sea lampreys is primarily influenced by external circumstances. In the presence of abundant food, the proportion of male lampreys tends to decrease. Conversely, in situations of food scarcity, the proportion of male lampreys increases.

The phenomenon of lampreys altering their gender ratios based on external environmental changes highlights the significance of studying species that can adjust their gender ratios according to resource availability. Such research provides valuable insights into the development of these species and their impact on ecosystems.

## 1.2 Problem Restatement

In this paper, we need to deal with the following tasks:

- **Task 1:** Establish a model to evaluate the impact of altering lampreys' sex ratio on the larger ecological system.
- **Task 2:** Develop a model to predict the influence of altering the sex ratio to the population of lampreys and analyse the advantages and disadvantages accordingly.
- **Task 3 :** Build several models to study the impact on the stability of the ecosystem considering the changes in the sex ratios of lampreys.
- **Task 4 :** Integrate data from other organisms in the ecosystem into the model to assess the advantages conferred to other species by changes in lamprey sex ratios.

## 1.3 Our Work

We made a flow chart to better represent our work.

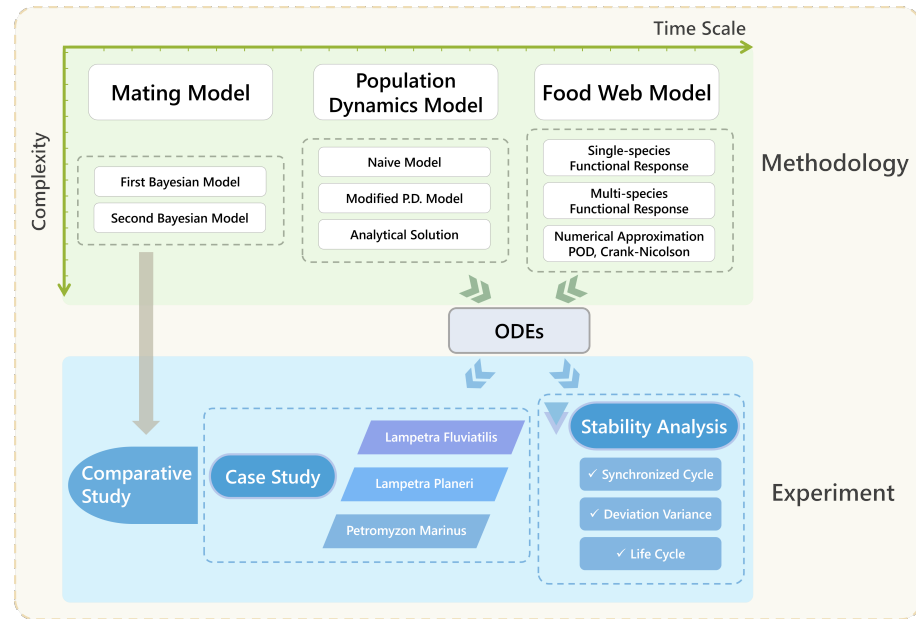


Figure 1: Flow chart of our work

## 2 Assumptions and Justifications

- **Assumption 1:** We assume that the lamprey population follows logistic growth.
- **Justification:** Through literature review[1], we deduce that the logistic model can better predict the growth of lamprey.
- **Assumption 2:** We assume that lampreys adopt one-to-one mating strategy.
- **Justification:** In the natural environment, we acknowledge that lampreys typically exhibit a polygynous mating system. However, to simplify the model, we assume a monogamous mating system for lampreys. This simplification is a common assumption in many studies investigating lamprey mating behavior.
- **Assumption 3:** The food web of lampreys is dominated by the hosts.
- **Justification:** As indicated in reference, the interplay between hosts and parasites assumes a pivotal role within the lamprey food web.
- **Assumption 4:** The estimation of both input and output energy for a given species can be derived through its overall size, a methodology that can similarly be applied to assess the accompanying ecosystem energetics.
- **Justification:** In ecosystems, trophic pyramids highlight the size-energy transfer connection. Physiological constraints and ecological models recognize size's impact on energy dynamics. Despite variations due to interspecies differences and environmental conditions, a species' size remains a key factor affecting its energy input and output, thus further correlating with indicators of one ecosystem.

### 3 Notations

Symbol	Definition	Unit
$N$	the number of lamprey population	/
$M$	the number of male lamprey population	/
$F$	the number of female lamprey population	/
$\theta_{m,f}$	successful mating rate	/
$T_{m,f}$	the number of mating attempts of one individual	/
$\alpha$	survival rate of eggs from one mating	/
$H_i$	the number of the i-th host population	/
$P_j$	the number of the j-th parasite population	/
$b$	birth rate of lamprey population	/
$d$	death rate of lamprey population	/
$S$	size of lamprey population	mm
$\Delta T$	grid size for large time scale model	decade
$\Delta t$	grid size for medium time scale model	month

### 4 Methodology

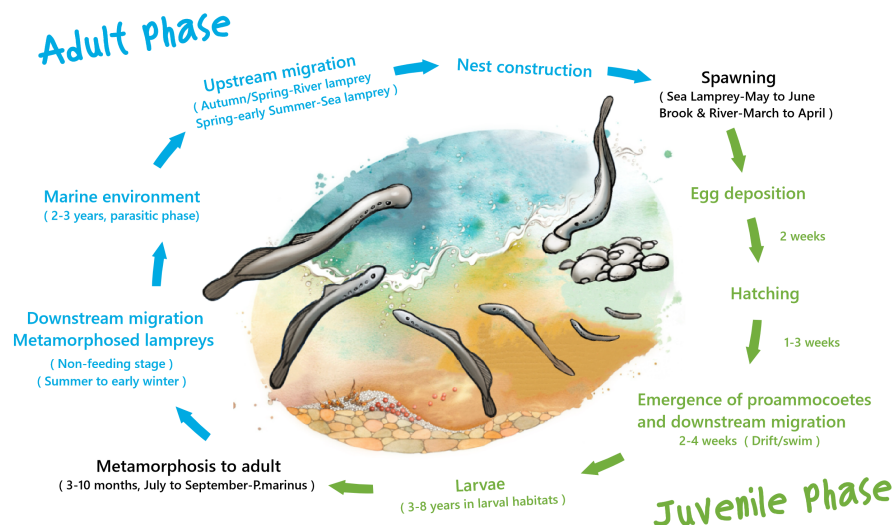


Figure 2: Schematic Diagram of the Lamprey Growth Cycle

The lamprey life cycle involves spawning in nests in clear streams, hatching into larvae that drift downstream and burrow into sediment to become filter feeders. After a metamorphosis phase, they make a transition into either freshwater-dwelling adults or anadromous adults that migrate to the sea, prey on other animals (depending on whether parasitic), and return to freshwater to spawn and die.

Reproduction involves nest-building, egg fertilization, and the subsequent death of both adults. Correspondingly, we characterize this life cycle by introducing the following models: **Population Dynamics (P.D. Model)**, **Mating Model (M. Model)** and the **Food Web Model (F.W. Model)**.

## 4.1 Large Lamprey Model (LLM)

As illustrated in Figure 3, we divide the LLM into three sub-models on large, medium, and small time scales. The M. Model investigates the impact of mating behavior on the population, corresponding to a small time scale, with a time span measured in days. The F.W. Model explores the effects of multiple hosts and parasites on the population, corresponding to a medium time scale, with a time span measured in months. Finally, the P.D. Model studies the impact of dynamic growth on the population, corresponding to a large time scale, with a time span measured in decades.

In the natural environment, empirical observations indicate that the reproductive cycle of lampreys spans approximately 15 to 40 days, with an average gestation period of approximately 6 months. Furthermore, the average lifespan of an individual lamprey is observed to fall within the range of 5 to 10 years. In practical implementation, as the time scale of the **M. Model** is relatively small in contrast to the other models, we assume it to be continuous. We define the time scale of the **P.D. Model** and the **F.W. Model** as the **Outer Iteration** and **Inner Iteration** respectively. Additionally, one Inner Iteration is developed within the smallest interval of the Outer Iteration.

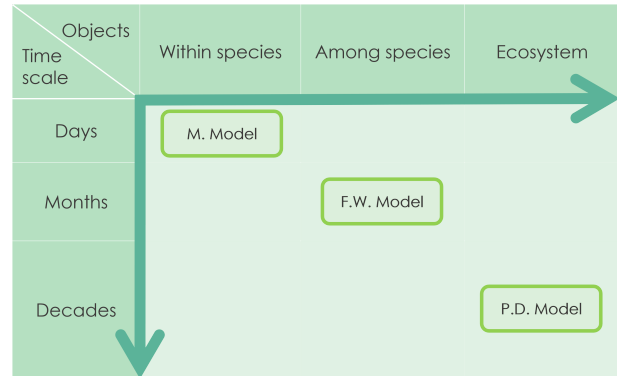


Figure 3: LLM Hub

## 4.2 Population Dynamics (P.D. Model)

### 4.2.1 Population Dynamics without Sex Variation

To begin with, we model the dynamic system with the naive growth model.

$$N(t+1) = N(t) + (b - d) \cdot N(t) \quad (1)$$

where b stands for the birth rate, d stands for the death rate and N(t) represents the number of lampreys at time t.

### 4.2.2 Population Dynamics with Sex Variation

We further characterize the male and female components of the lamprey community.

$$\begin{aligned} M(t+1) &= M(t) + p \cdot (b - d) \cdot N(t) \\ F(t+1) &= F(t) + (1 - p) \cdot (b - d) \cdot N(t) \\ N(t) &= M(t) + F(t) \end{aligned} \quad (2)$$

where  $M(t)$  stands for the number of males,  $F(t)$  for the number of females and  $p$  stands for the probability of developing as a male.

### 4.3 Mating Model (M. Model)

The mating behavior of lampreys has been previously studied using mathematical distributions within the confined timeframe of the breeding season[2]. Lampreys exhibit temporal variations in sexual selection due to changes in the operational sex ratio (OSR) during different breeding phases. These phases include a nest-building phase with most females, a spawning phase with a prevalence of males, and a return to an excess of females towards the end of the season, resulting in a highly polygynandrous system. In this study, we investigated the effects of the lamprey mating system on birth rate. According to the work [2], we estimated pre-copulatory sexual selection throughout the breeding season and employed fitness variance-based approaches to assess the strength of sexual selection. Two Bayesian models were then utilized to examine the mechanisms of selection on traits, including body size and temporal spawning pattern. By integrating trait-based measures of sexual selection, we aimed to elucidate the factors influencing mating success. This model contributes to understanding the intricate interplay between sexual selection, mate choice, and individual phenotypic characteristics within lamprey mating dynamics.

#### 4.3.1 Birth Rate Resulting from Mating System

Mating systems are confirmed as the major contributor to the birth of species, thus we first design the general form of successful mating times, which is characterized by two distributions sequentially. The mathematical relationship can be further characterized by Equation 3.

$$\begin{aligned} A_{m,f,t} &\sim \text{Poisson}(T_{m,f,t}) \\ C_{m,f,t} &\sim \text{Binomial}(A_{m,f,t}, \theta_{m,f,t}) \end{aligned} \quad (3)$$

where  $\text{Poisson}(\bullet)$  denotes the Poisson distribution, and  $\text{Binomial}(\bullet)$  denotes the Binomial distribution. The first three-dimensional array  $A_{m,f,t}$  stands for the total number of matings between each male and female, and the second three-dimensional array  $T_{m,f,t}$  represents the number of mating attempts of one individual and the third three-dimensional array  $\theta_{m,f,t}$  denotes the success rate of one mating, which is followed by the implicit constraint  $\theta_{m,f,t}^{i,j,k} \in [0, 1]$ . And  $C_{m,f,t}$  denotes the successful mating times.

With a few minutes of careful calculation, we finally work out the experience of the snapshot matrix  $C_{m,f,t=t_0}$  at time  $t_0$ :

$$\begin{aligned} \mathbb{E}(C_{m,f}) &= \sum_{k=1}^{+\infty} \mathbb{P}(C_{m,f} = k) \cdot k \\ &= \lim_{n \rightarrow \infty} \sum_{k=1}^n \binom{n}{k} \cdot A_{m,f}^k \cdot \theta_{m,f}^{n-k} \cdot k. \\ &= \theta_{m,f} \cdot \left( \lim_{n \rightarrow \infty} \sum_{k=1}^n e^{-T_{m,f}} \cdot \frac{(T_{m,f})^k}{(k!)} \right) \cdot T_{m,f}. \\ &= \theta_{m,f} \cdot T_{m,f} \end{aligned} \quad (4)$$

We can further get the birth rate by multiplying the survival coefficient by the experience of the successful mating times.

$$b = \alpha \cdot \mathbb{E}(C_{m,f}) = \alpha \cdot \theta_{m,f} \cdot T_{m,f} \quad (5)$$

In actuality, the coefficient  $\alpha$  delineates the survival rate of eggs transitioning from successful mating to the juvenile phase, encompassing factors such as predation by fish or invertebrates, competition for resources, physical disturbances like water flow or sedimentation, and the conceivable influence of pollutants or toxins within the ambient environment.

#### 4.3.2 First Bayesian Model Based on Sexual Selection

Symbol	Definition	Unit
$S_m$	male size	mm
$S_f$	female size	mm
$OSR_t$	ratio of receptive male to female	mm
$CSM$	average male size	mm
$CSF$	average female size	mm
$S_m$	male size	mm
$RP_{m,t}$	reproductive period of male	day
$RP_{f,t}$	reproductive period of female	day
$r_{1,m}$	random male effects (individual) for uncontrolled source of variation	/
$r_{1,f}$	random female effects (individual) for uncontrolled source of variation	/

In this section, we present our first Bayesian model that focuses on the role of sexual selection in mating dynamics. The first Bayesian model employs a daily time-step analysis of mating interactions, and was designed to investigate the influence of daily variations in the social environment (e.g., operational sex ratio, size of current competitors) on the two processes contributing to mating success: the number of mating attempts  $T_{m,f,t}$  and the rate of successful mating  $\theta_{m,f,t}$ . We hypothesized that larger males and females would exhibit higher mating success, as body size generally affects intrasexual mate competition [3]. Additionally, we anticipated a higher probability of successful mating in pairs of similar size, based on the possibility of size-assortative mating in lampreys as suggested by [4].

Furthermore, we predicted interactive effects between individual phenotype and the social environment, where the positive impact of body size on mating success would be more pronounced in a more competitive environment. In this manner, we incorporate parameters such as individual phenotypic traits, social environment factors, and the dynamics of mating acts to understand how sexual selection influences mating patterns. By considering factors like body size, size difference between partners, operational sex ratio, and time since the start of the reproductive period, we aim to quantify the effects of these variables on the number of mating attempts and the probability of successful matings. This relationship can be further demonstrated as follows (definition of notations used can be found in Table 7 and *inv.logit* denotes the inverse function of the logistic function):

$$T_{m,f,t} = \exp \left( \begin{array}{l} \alpha_1 + \beta_1 S_m + \beta_2 S_f + \beta_3 \text{abs}(S_m - S_f) + \beta_4 \text{OSR}_t + \beta_5 (S_m * \text{OSR}_t) \\ + \beta_6 (S_f * \text{OSR}_t) + \beta_7 (\text{CSM}_t - S_m) + \beta_8 (\text{CSF}_t - S_f) + \beta_9 \text{RP}_{m,t} \\ + \beta_{10} \text{RP}_{f,t} + r_{1,m} + r_{1,f} \end{array} \right) \quad (6)$$

$$\theta_{m,f,t} = \text{inv. logit} \left( \begin{array}{l} \alpha_2 + \beta_{11} S_m + \beta_{12} S_f + \beta_{13} \text{abs}(S_m - S_f) + \beta_{14} \text{OSR}_t + \\ \beta_{15} (S_m * \text{OSR}_t) + \beta_{16} (S_f * \text{OSR}_t) + \beta_{17} (\text{CSM}_t - S_m) + \\ \beta_{18} (\text{CSF}_t - S_f) + \beta_{19} \text{RP}_{m,t} + \beta_{20} \text{RP}_{f,t} + r_{2,m} + r_{2,f} \end{array} \right)$$

#### 4.3.3 Second Bayesian Model based on Identified Traits

Symbol	Definition	Unit
$r_{2,m}$	random effect	/
$r_{2,f}$	random effect	/
$I_m$	mating activity first date of male	/
$I_f$	mating activity first date of female	/
$D_m$	duration of mating activity of male	s
$D_f$	duration of mating activity of female	s

In this subsection, we introduce another Bayesian model that focuses on the influence of specifically identified traits on mating dynamics, aiming to explore whether the processes leading to mating success were influenced by temporal characteristics of mating activities subjecting to selection. We hypothesized that individuals initiating mating early in the season and spreading their mating efforts over a longer period would have a higher number of mating attempts. Furthermore, we investigated the interaction between body size and the temporal distribution of mating activity, as the fitness benefits of adopting specific temporal patterns may depend on individual phenotype. For example, smaller individuals may compensate for their lower competitive ability by concentrating their mating activity within a shorter timeframe.

In the study [2], the authors investigate the effects of individual phenotypic traits, such as body size, on the number of mating attempts and the probability of mating success. By examining the relationships between these traits and mating outcomes, the authors aim to identify which traits play a significant role in determining mating success. This model provides insights into the relative importance of different traits in driving mating patterns, allowing us to better understand the selective forces acting on individuals within a population. The math model can be further refined as the following Equation 7, (definition of notations used can be found in Table 8 and *inv.logit* denotes the inverse function of logistic function).

$$T_{m,f} = \exp \left( \begin{array}{l} \alpha_1 + \beta_1 S_m + \beta_2 S_f + \beta_3 \text{abs}(S_m - S_f) + \beta_4 I_m + \beta_5 I_f + \\ \beta_6 D_m + \beta_7 D_f + \beta_8 (S_m * I_m) + \beta_9 (S_f * I_f) + \beta_{10} (S_m * D_m) \\ + \beta_{11} (S_f * D_f) + r_{1,m} + r_{1,f} \end{array} \right) \quad (7)$$

$$\theta_{m,f} = \text{inv. logit} \left( \begin{array}{l} \alpha_2 + \beta_{12} S_m + \beta_{13} S_f + \beta_{14} \text{abs}(S_m - S_f) + \beta_{15} I_m + \beta_{16} I_f + \\ \beta_{17} D_m + \beta_{18} D_f + \beta_{19} (S_m * I_m) + \beta_{20} (S_f * I_f) + \beta_{21} (S_m * D_m) \\ + \beta_{22} (S_f * D_f) + r_{2,m} + r_{2,f} \end{array} \right)$$

We should also note that, in the practical calculation, we use the **Multiple Linear Regression (MLR)** [12] to generate the coefficients in Equation [6; 7]

## 4.4 Modified Population Dynamic Model Considering the Mating System

### 4.4.1 Setup of the Dual Logistic Model

In the context of lamprey population dynamics, a modified model is proposed that incorporates the mating system's influence. The modified model adopts a **dual logistic framework** to capture the interactions between reproductive processes and population growth. One logistic curve represents the reproductive output, incorporating factors such as mating success, fecundity, and survival rates of eggs and larvae. The other logistic curve describes the population growth rate, considering factors such as mortality rates, resource availability, and environmental conditions. By integrating the mating system into the population dynamic model, a more accurate representation of lamprey population dynamics can be achieved, considering the influence of reproductive processes on population growth and persistence.

$$\begin{cases} M(t+1) - M(t) = p \cdot [b - d(M+F)](M+F) \\ F(t+1) - F(t) = p \cdot [b - d(M-F)](M-F) \\ \mathbf{L}(t) = [M(t), F(t)]^\top \end{cases} \quad (8)$$

$$\Rightarrow \begin{cases} \nabla_t(M(t) + F(t)) = 2p \cdot M(t)[b - d(M(t) + F(t))] \\ \nabla_t(M(t) - F(t)) = 2p \cdot F(t)[b - d(M(t) - F(t))] \end{cases} \quad (9)$$

$$\Rightarrow \begin{cases} \nabla_t(A \cdot \mathbf{L}(t)) = p \cdot (2b \cdot \mathbf{L}(t) - 2d \cdot \mathbf{L}^\top(t) \cdot \mathbf{L}(t) \cdot \mathbf{1}) \\ A = \begin{bmatrix} 1 & 1 \\ 1 & -1 \end{bmatrix} \\ \mathbf{L}(t) = [M(t), F(t)]^\top \\ \mathbf{1} = [1, 1]^\top \end{cases} \quad (10)$$

### 4.4.2 Solution to the Dual Logistic Model

With the knowledge of Ordinary Differential Equations, our detailed solution is presented as follows:

$$\begin{aligned} \frac{\Delta \mathbf{L}(t)}{2b \cdot \mathbf{L}(t) - 2d \cdot \mathbf{L}^\top(t) \cdot \mathbf{L}(t) \cdot \mathbf{1}} &= p \cdot A^{-1} \Delta t \\ \Rightarrow \begin{cases} L(t) = \frac{b}{d} \left( I_2 + e^{c \cdot p \cdot A^{-1} t} \right)^{-1} \cdot e^{c \cdot p \cdot A^{-1} t} \cdot \mathbf{1} \\ b = \alpha \cdot \mathbb{E}(C_{m,f}) = \alpha \cdot T_{m,f} \cdot \theta_{m,f} \end{cases} & \quad (11) \end{aligned}$$

where  $c$  represents the integration constant and  $e^{c \cdot p \cdot A^{-1} t}$  stands for the matrix exponential, with  $c, p, t$  scalars and  $A^{-1}$  the inverse of matrix  $A$  mentioned in Equation 10.

## 4.5 Food Web Model (F.W. Model)

In this section, we model the behavior of multiple hosts and parasites. We should also note that this model is based on the medium time scale, as demonstrated in section 4.1.

### 4.5.1 Single Species Functional Response

Population growth in a food web is predominantly governed by the resource acquisition rate of a species, while population decline is primarily influenced by predation rate, as well as metabolic processes and natural mortality. Consequently, accurately simulating population dynamics necessitates an understanding of the rate at which species acquire resources or engage in predation. Typically, this rate is characterized by a functional response function, as originally proposed by [8]. In the context of lampreys, comprehending their resource acquisition and predation rates, as described by the functional response function, is fundamental for studying their population dynamics within the food web.

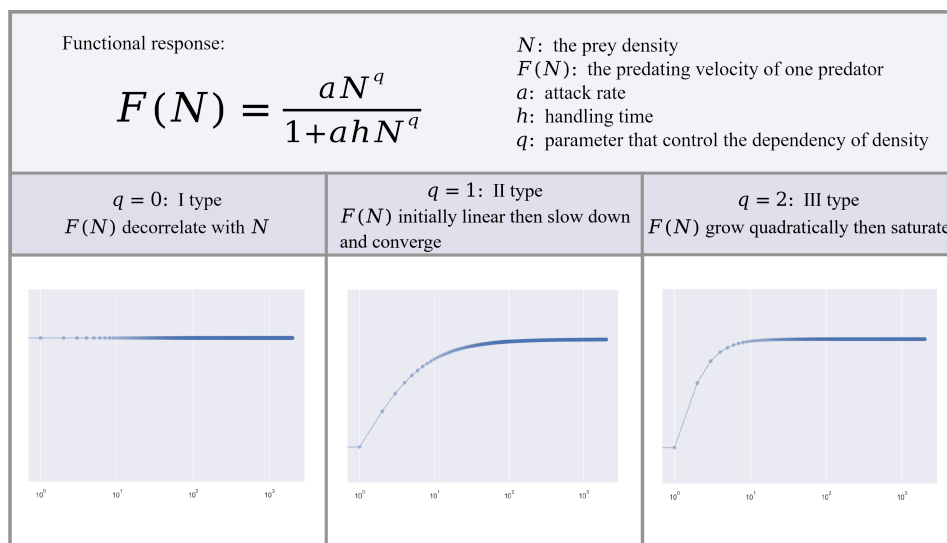


Figure 4: Three functional responses

where  $N$  represents prey density,  $F(N)$  represents the predation rate of an individual predator,  $a$  represents the attack rate of the predator, and  $h$  represents the handling time required to process a prey item.  $q$  is a parameter that regulates the density-dependent form. When  $q = 0$ , the predation rate  $F(N)$  is a constant independent of prey density  $N$ , referred to as a **Type I** functional response. When  $q = 1$ ,  $F(N)$  increases linearly with  $N$  at low densities and then saturates at a certain level, known as a **Type II** functional response. When  $q = 2$ ,  $F(N)$  increases quadratically with  $N$  at low densities and then saturates, also known as a **Type III** functional response. Many researchers have analyzed the relationship between prey density and predation rate and have found that many systems follow a Type II functional response [8].

### 4.5.2 Multispecies Functional Response

We employ a series of **Ordinary Differential Equation (ODE)** characterizing the relationship between the host and the parasites. We numerically investigate the behavior of the host-parasite interaction system with type-II functional response for  $n$  hosts and  $n$  parasites and the function is presented as follows:

$$\begin{aligned}\frac{dH_i}{dt} &= \left( r_i \left( 1 - \frac{\sum_{k=1}^n \varphi_{ik} H_k}{K} \right) - \sum_{k=1}^n \frac{\alpha_{ik}}{1 + \sum_{\ell=1}^n \beta_{ik} H_{\ell}} P_k \right) H_i \\ \frac{dP_j}{dt} &= \left( \sum_{k=1}^n \frac{c_{kj} \alpha_{kj}}{1 + \sum_{i=1}^n \beta_{ki} H_i} H_k - d_j \right) P_j\end{aligned}\quad (12)$$

where  $i, j = 1, 2, \dots, n$ ,

- $H_i$ : The population number of the i-th host.
- $P_j$ : The population number of the j-th parasite.
- $r_i$ : The basal growth rate of host i
- $d_j$ : The death rate of parasite j
- $K$ : The carrying capacity of hosts
- $\varphi_{ik}$ : Competitive ability between hosts
- $c_{ij}$ : Competitive ability between host-to-parasite conversion due to host utilization
- $\beta_{ik}$ : Energy allotment of parasites to other host type

We should note that  $\alpha$  denotes the parasitism efficiency. To simulate the alternating dominance phenomenon, according to the paper [6], we set the parasitism efficiency matrix  $A = [\alpha_{ij}]$  to be diagonally dominant, such that:

$$\alpha_{ii} \geq \sum_{j \neq i} \alpha_{ij}, \forall i \quad (13)$$

#### 4.5.3 Numerical Approaches to Solve the Response ODEs

In this section, we focus on conquering each Inner Iteration mentioned in Section 4.1. In order to solve the complex nonlinear system characterized by Equation 12, our team first set up the classical condition for the numerical **Finite Difference Method** [7]. Notably, as we are solving the multi-dimensional ODEs, we modify the storage mechanism of the target matrix and the intermediate vectors.

In Figure 5, the lower-left and upper-right corners represent values determined based on the P.D. model. Consequently, the x-axis corresponds to the smallest granularity of the P.D. model, specifically the length of each Outer Iteration. Thus, the P.D. model can be conceptualized as piecewise from the perspective of medium size. Conversely, the oscillating climbing blue line denotes the solution derived from the F.W. model, which, intuitively, adheres to the Lipsitz condition within the neighbourhood. The Inner

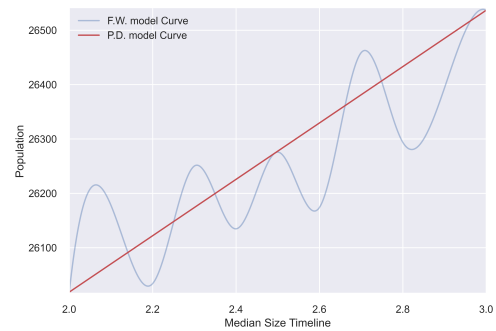


Figure 5: Scheme of Inner Iteration within one large scale time interval

Iteration problem involves solving Equation 12 with the P.D. model results serving as the initial condition, encompassing three major steps:

- Step 1: Setup of the general form of finite difference condition

For computation convenience, we note the host and parasite population as the column stack of the vectors from  $T_j$  to  $t$ :

$$\begin{aligned} H^t &= [H(T_j), H(T_{j+\Delta t}) \dots H(t)] \\ P^t &= [P(T_j), P(T_{j+\Delta t}) \dots P(t)]. \end{aligned} \quad (14)$$

In this manner, we restate the Multispecies Functional Response Equation 12 as follows:

$$\frac{d}{dt} \begin{bmatrix} H^t \\ P^t \end{bmatrix} = f \left( \begin{bmatrix} H^t \\ P^t \end{bmatrix} \right) \quad (15)$$

Subject to the initial conditions:

$$\left\{ \begin{array}{l} H(t = T_j) = [H_1^{T_j}, H_2^{T_j} \dots H_n^{T_j}]^\top \\ P(t = T_j) = [P_1^{T_j}, P_2^{T_j} \dots P_n^{T_j}]^\top \\ H(t = T_{j+1}) = [H_1^{T_{j+1}}, H_2^{T_{j+1}} \dots H_n^{T_{j+1}}]^\top \\ P(t = T_{j+1}) = [P_1^{T_{j+1}}, P_2^{T_{j+1}} \dots P_n^{T_{j+1}}]^\top \end{array} \right. \quad (16)$$

- Step 2: Decoupling of the nonlinear operator.

We initially collect the  $N$  snapshots of the vector  $[H^{T_j}, P^{T_j}]^\top_{j \in \{1, 2, \dots, N_T\}}$ , then compute the approximate linear operator  $K$  for the problem as follows:

$$f \left( \begin{bmatrix} H^t \\ P^t \end{bmatrix} \right) \cong K \begin{bmatrix} H^t \\ P^t \end{bmatrix} \quad (17)$$

where  $K$  is computed by:

$$K = f \left( \begin{bmatrix} H^t \\ P^t \end{bmatrix} \right) \cdot \left( \begin{bmatrix} H^t \\ P^t \end{bmatrix}^\top \begin{bmatrix} H^t \\ P^t \end{bmatrix} \right)^{-1} \begin{bmatrix} H^t \\ P^t \end{bmatrix}^\top \quad (18)$$

Then we implement the **Proper Orthogonal Decomposition (POD)** [9] to the operator  $K$ :

$$K = T^{-1} D T \quad (19)$$

then the ODE is of the form:

$$\frac{d}{dt} \left( T \begin{bmatrix} H^t \\ P^t \end{bmatrix} \right) = D \left( T \begin{bmatrix} H^t \\ P^t \end{bmatrix} \right) \quad (20)$$

where  $T$  is the eigenvector matrix and  $D$  denotes the eigenvalue matrix, which is diagonal and thus the linear transformed system is decoupled. This process is often referred to as **Jacobi Diagonalization**.

- Step 3: Discretization and derivative approximation

We first discretize the ODE obtained above in Equation 20 via the one-step method. As our problem is to model on a relatively small step scale and requires numerically stable results, we solve with the help of the **Crank-Nicolson Method**

$$\begin{bmatrix} H^{t+\Delta t} \\ P^{t+\Delta t} \end{bmatrix} = \begin{bmatrix} H^t \\ P^t \end{bmatrix} + \frac{\Delta t}{2} \cdot \left( K \begin{bmatrix} H^t \\ P^t \end{bmatrix} + K \begin{bmatrix} H^{t+\Delta t} \\ P^{t+\Delta t} \end{bmatrix} \right) \quad (21)$$

## 4.6 Model Evaluation

To evaluate the total size of one lamprey population, we announce the equation as follows:

$$S_{tot}(t) = S_m \cdot M(t) + S_f \cdot F(t) + (b - d) [pS_{lm}(t) + (1 - p)S_{lf}(t)] \quad (22)$$

where  $S_{tot}$  stands for the total size of the lamprey,  $S_m, S_f$  represent the size of male and female adult lamprey respectively,  $S_{lm}, S_{lf}$  stands for the mean size of larval lamprey and  $p$  stands for the probability of larval lampreys altering sex to male.

By the hypothesis above, we assume that larval lamprey grows logistically and the average size of the lamprey is the integration average of the logistic function, with the final asymptote value equal to the average adult lamprey size. Thus,  $S_{lm}$  can be computed as follows:

$$S_{lm} = \frac{S_m}{\Delta T} \int_{t_0}^{t_0 + \Delta T} \text{Logit}(t) dt \quad (23)$$

where Logit denotes the logistic function, and  $S_{lf}$  can be computed in the same manner.

Then, we evaluate the impact of the lamprey population on various aspects of ecosystem dynamics, focusing on ecosystem function, empowerment, and integrity, according to the Odum Theory [13] proposed by the Nobel Prize nominator H.T Odum:

- a) Ecosystem Function:

The ecosystem function, denoted as  $E_{func}$ , is intricately tied to the population dynamics and total size of lampreys. A logical model can be expressed through the logistic growth equation:

$$E_{func} = \frac{K \cdot C_1}{C_1 + K} \cdot S_{tot} \quad (24)$$

where  $K$  represents the carrying capacity of the ecosystem,  $P$  is the lamprey population, and  $S_{tot}$  is the total size of the lamprey population.

- b) Ecosystem Empowerment:

Ecosystem empowerment, denoted as  $E_{empower}$ , reflects the ecological vigour facilitated by the lamprey population and its total size. A straightforward model is given by:

$$E_{\text{empower}} = C_2 \cdot S_{\text{tot}} \quad (25)$$

This model underscores the idea that the empowerment of the ecosystem is intricately linked to both the abundance and size of the lamprey population.

### c) Ecosystem Integrity:

Ecosystem integrity, represented as  $E_{\text{integrity}}$ , is impacted by the balance between the lamprey population and its total size. A balanced ratio is crucial for optimal ecosystem integrity, as indicated by the model:

$$E_{\text{integrity}} = \frac{C_3}{S_{\text{tot}}} \quad (26)$$

This equation suggests that maintaining a proportional relationship between the lamprey population and its total size contributes to the overall integrity of the ecosystem.

In summary, the models presented here offer a concrete and logical representation of how the population and total size of lampreys influence ecosystem function, empowerment, and integrity. Adjustments to these models can be made based on empirical data and specific ecological contexts.

## 5 Numerical Results

### 5.1 Preparation

#### 5.1.1 Case study: Setup of Three Representative Specimens

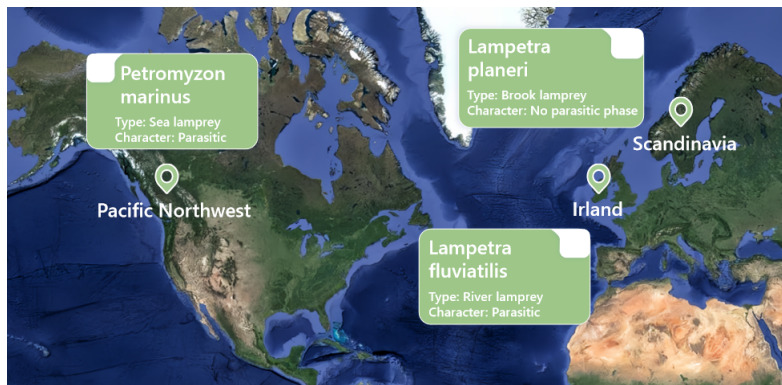


Figure 6: Distribution and character of three representative specimens

According to general principles, we have selected the three lamprey species that are most representative in terms of characteristics and quantity as our primary subjects of study. The main gathering areas for these three lamprey species are distinct. Among them, *Lampetra planeri*, commonly known as the Brook Lamprey, represents a species with characteristics suitable for studying smaller riverine ecosystems. *Petromyzon marinus*, or the Sea Lamprey, has garnered attention due to its significant ecological roles in both freshwater and marine environments. Lastly, *Lampetra fluviatilis*, known as the River Lamprey, has been chosen for its dominant presence in riverine systems. The selection of these three most representative lamprey species not only encompasses different aquatic environments but

also captures the diversity within the lamprey taxon. The distribution and characteristics comparison of the three species is illustrated in Figure 7.

	Petromyzon marinus	Lampetra planeri	Lampetra fluviatilis
Larvae	fine particulate matter - mainly microorganisms and detritus		
Food			
Adults	basking shark, sturgeon, shad, herring, atlantic salmon, atlantic cod, haddock, atlantic mackerel, pollock, hake, swordfish, striped bass	do not feed at all	bluefish, smelt, sprat, baltic herring, powan, sea trout, shad, flounder
Predator	Phoxinus spp, Anguilla spp, Artedielius spp, Perca spp, Cottus spp		

Figure 7: Comparison of three lamprey species

### 5.1.2 Comparative Study: Comparison of two Bayesian Mating Models

To implement the comparative study, we get the coefficients in Equation 6 and 7, with the help of **Multiple Linear Regression (MLR)**. Experiments are done on the data acquired in the study [2], where the authors get the data from the European lampreys residing in the river.

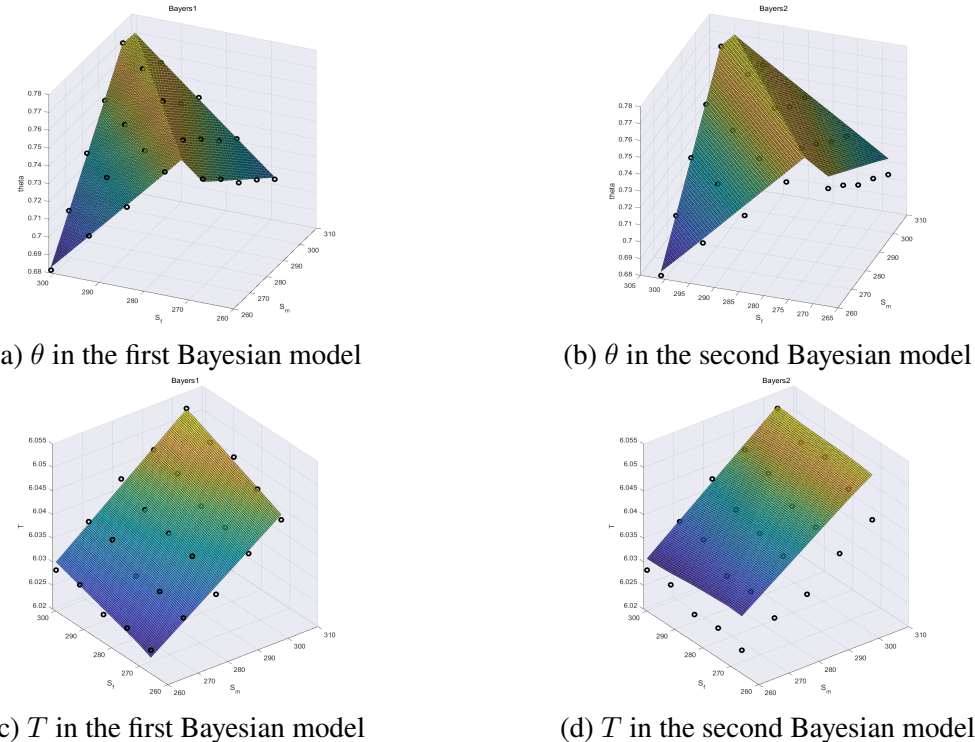


Figure 8: Comparison of two Bayesian mating models

As depicted in Figure 8, the first and second Bayesian models exhibit an ascending trend in the successful mating rate  $\theta$  as both male and female sizes increase, aligning with the size coupling strategy

observed in lampreys. Notably, the female size demonstrates a more pronounced incline, corresponding to the findings of the author [11]. The quantity of mating attempts demonstrates a consistent augmentation concerning the sizes of both males and females. While the first model adeptly captures the nuances of the training data, conversely, the second model exhibits poor performance at the extremities. Consequently, we utilize the first model in subsequent experiments.

### 5.1.3 Parameter Choice and Numerical Simulation

In the numerical experiment, we fix a few parameters which are stated below:

- Choices of parameters of three species:

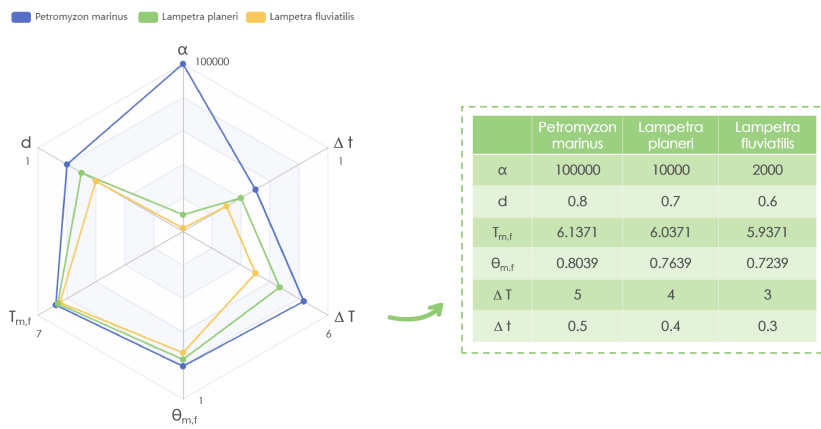


Figure 9: Comparison of data for three species

According to the specific characterization of the three species, we design the parameters as illustrated in Figure 9. Additionally, we simulate the lamprey population with sex ratio alteration and without sex ratio alteration by setting the male-altering possibility to 0.78 and 0.5 respectively (as mentioned in the question, we choose the possibility when the food availability is low).

- Choices of competitive coefficients in Food Web model:

Due to the lack of real data on the three lamprey populations and for the simplicity of our simulation, we generate  $\alpha, \beta, \phi, c, r, d$  as follows:

$$\alpha = \text{eye}(3) + \text{rand}(3, 3) \cdot (\text{ones}(3, 3) - \text{eye}(3)) \quad (27)$$

$$\beta = \text{rand}(3, 3), \quad \phi = \text{rand}(3, 3), \quad C = \text{rand}(3, 3) \quad (28)$$

$$\text{Vector D} = \text{rand}(3, 1), \quad \text{Vector R} = \text{rand}(3, 1) \quad (29)$$

where  $\text{rand}(n, m)$  generates an  $n \times m$  matrix with random values uniformly distributed in the range  $[0, 1]$ ,  $\text{eye}$  denotes the identical matrix.

These operations result in matrices and vectors with random values, creating a set of diverse and stochastic elements for further analysis, so it is crucial to emphasize that, we choose to simulate the competitive coefficients 500 times and take the mean of the results. We should also note that the following simulation is conducted based on the assumption that the three specimens are competitors and thus the system is 3-dimensional.

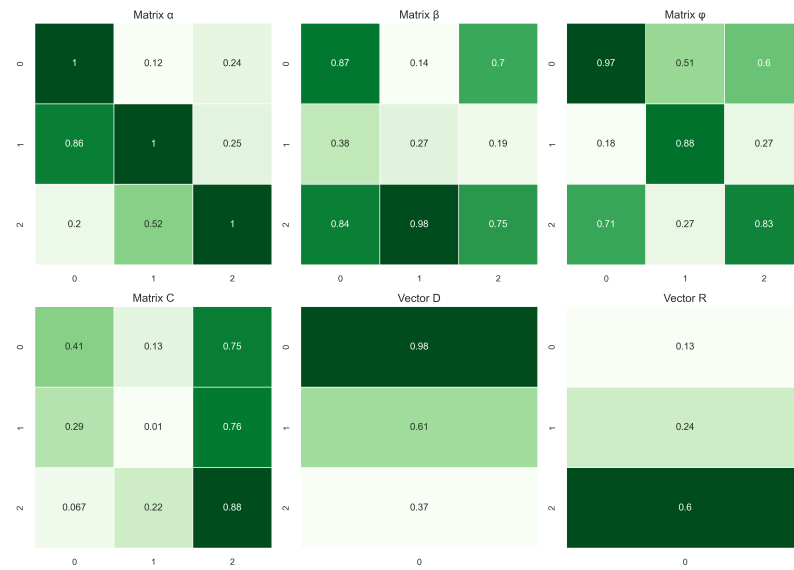


Figure 10: Heatmaps of Different Parameters

- Simulation Process and Equipment Dependency:

In the course of our numerical simulation endeavours, we leverage the capabilities of MATLAB and Python, two robust programming tools. To execute this digital exploration, our computational resources are anchored in the MacBook Pro, featuring the advanced M2 ultra chip. This high-performance hardware empowers us not only to model and solve ordinary differential equations (ODEs) but also to generate compelling visualizations using the Echart.

## 5.2 Responses to the Questions

### 5.2.1 Impact on the Larger Ecological System Given Sex Alteration

In this section, we investigate the ecological consequences of inducing food scarcity by manipulating the male-changing probability to 0.78. The numerical outcomes of this simulation, specifically concerning ecosystem function, empowerment, and ecosystem integrity at the culmination of day 2, are presented and analyzed.

		Ecosystem Functionality			Ecosystem Empowerment			Ecosystem Integrity		
		LP	LF	PM	LP	LF	PM	LP	LF	PM
Mean	with sex change	62.30074665	1039.193545	9116.613802	5329.555588	86947.10006	760321.9787	0.973522308	0.088851145	0.007871613
	without sex change	60.37125075	717.9874776	6149.161922	4626.217355	68830.76617	677225.7955	0.440064257	0.056879765	0.004856127
Variance	with sex change	5.77379081	5.150349442	5.196137242	5.68859968	5.970659021	6.277461328	6.452143874	5.280374119	5.810708418
	without sex change	6.052982388	5.874372281	5.774816721	5.061820553	7.375314519	5.370877296	6.733745315	5.706478307	6.259879186
Conditional number	with sex change	11.20469816	12.99322316	13.62506847	13.95287951	16.12129252	14.97977358	15.276428	12.92292731	13.97353713
	without sex change	13.79362243	14.3824632	12.74086871	13.7382191	16.89342686	17.83945606	16.70175112	16.78887053	16.18784135

Figure 11: Three major indicators of one ecosystem

The obtained data is summarized in Table 12, where we observe variations in ecosystem metrics under altered conditions. Subsequently, the impact of simulated food scarcity on day 2 is reflected in  $E_{\text{func}}$ ,  $E_{\text{empower}}$ , and  $E_{\text{integrity}}$ . Where the conditional number denotes the error propagation rate of each evaluation function defined by  $CN = f(\delta S_{\text{tot}})/\delta S_{\text{tot}}$

The observed changes in these metrics shed light on the nuanced dynamics of the existence of a sex alteration mechanism and also illustrate the tiny nuance caused by the different initial conditions for each specimen.

After introducing the sex ratio change mechanism, the ecosystem functionality slightly augments, the empowerment boosts and ecosystem integrity declines. In a word, given sex alteration, all the indicators of the ecosystem perform better.

### 5.2.2 Advantages and Disadvantages of Sex Alteration on Lamprey Population

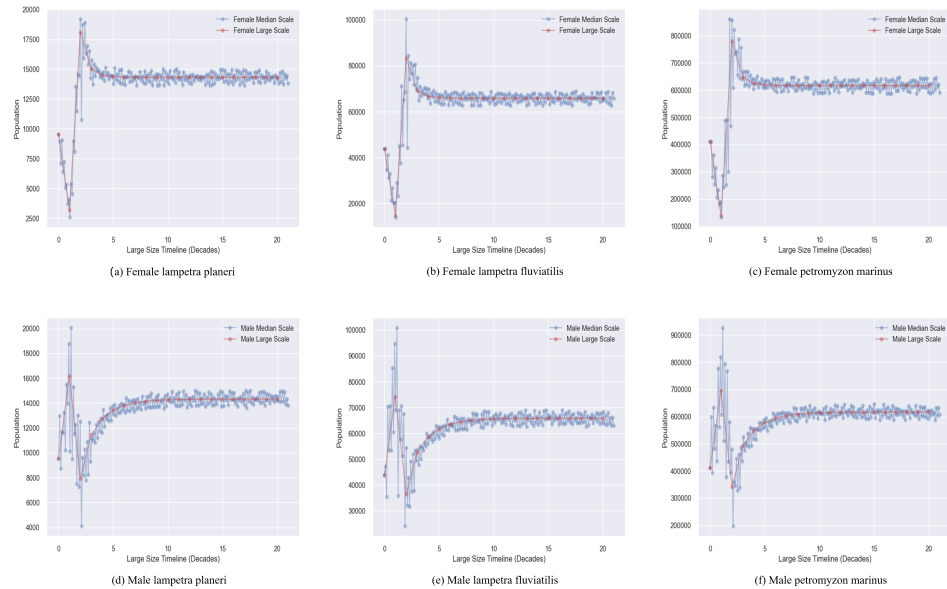


Figure 12: Male and Female population dynamics with sex alteration

Figure 12 depicts the variations in lamprey population at different time scales when the sex ratio of lampreys changes with external conditions. We observe that when the sex ratio of lampreys undergoes alterations due to external conditions, the trends among three different lamprey types are roughly similar. Specifically, the female lamprey experiences a rapid decline followed by a quick increase in a short period, then followed by a slow decline until it levels off. Conversely, the male lamprey exhibits an opposite trend. Additionally, it is noted that when there is a significant fluctuation in the sex ratio at a large scale, the fluctuations at the medium scale also increase. This is also reflected in the deviation variance, as shown in Figure 15.

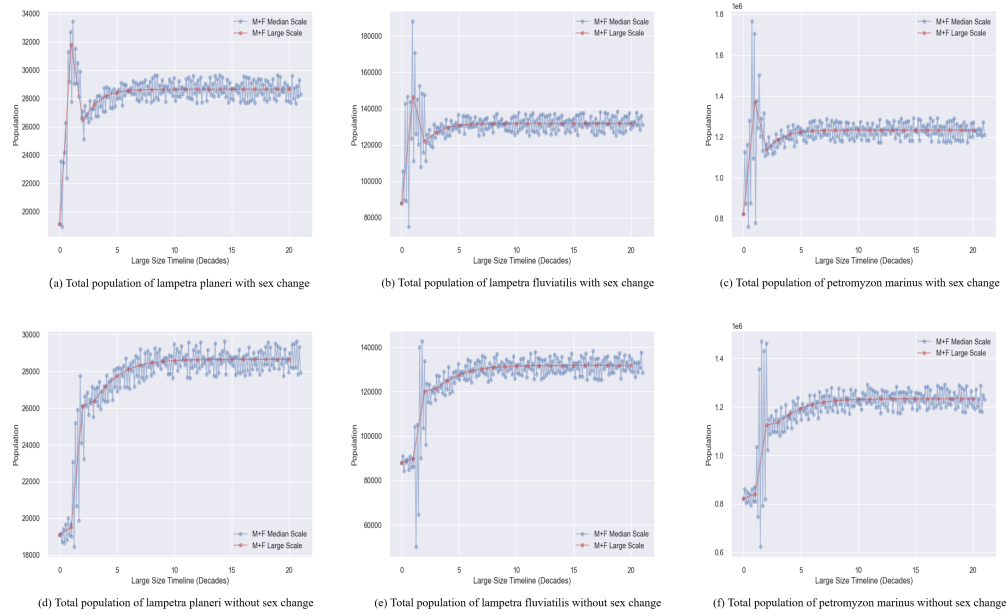


Figure 13: Lamprey population dynamics comparing the sex changing condition

To better assess the advantages and disadvantages of sex alteration, we predicted the population of females and males for three lamprey species with and without sex change, as shown in Figure 13. We observe that, in situations where the sex ratio undergoes alterations, the total population of lampreys experiences a rapid increase followed by a swift decline before gradually growing until it stabilizes. Conversely, in cases where the sex ratio remains constant, both males and females exhibit slow growth until reaching stability, and the total population follows a similar trend.

Therefore, we can infer that altering the sex ratio allows lampreys to rapidly expand their population in the short term, securing a competitive advantage in resource utilization. Furthermore, changes in the sex ratio enhance species adaptability, enabling a swift response to environmental shifts, thereby capitalizing on favorable ecological conditions in the short term. The disadvantages include a rapid decrease in population within a specific timeframe, and in the short term, there are larger fluctuations in population at both the medium and large scales. The sharp population fluctuations may have adverse effects on the ecosystem in the short term.

### 5.2.3 Impact on the Stability of Ecological System Given Sex Alteration

Here are a few practical metrics that depict the impact of sex ratio change on the ecosystem.

- Metric 1: Synchronized Cycle of parasites and hosts:

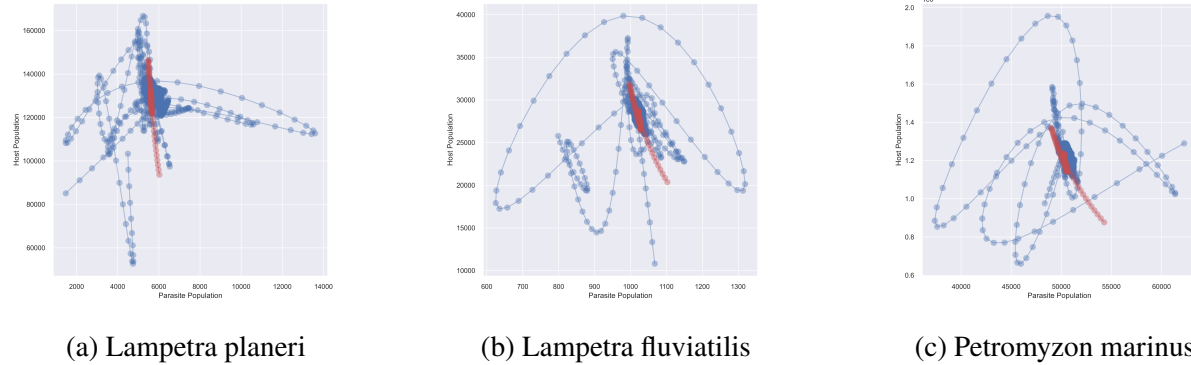


Figure 14: Relations between parasite population and host population

In exploring the behavior of a three-dimensional system described by Equation 12, we plot the synchronized phase scheme of the host-to-parasite relationship in Figure 16 in blue lines. Additionally, we also plot the large time scale model (red lines), which indicates the general direction of the development of the lamprey species. Stable points have been identified at coordinates  $(5.9e3, 1.3e5)$ ,  $(1.02e4, 2.8e4)$ , and  $(5e4, 1.2e6)$ . These stable points, find resonance with chaotic phenomena in the natural world. A review of the literature [10] published in Nature Journal underscores the prevalence of stable points, stable cycles, and chaotic behavior in second or higher-order difference equations, particularly those representing interactions between two or more species. The literature further notes that the onset of chaotic behavior often necessitates less severe nonlinearities. This intriguing insight suggests that a three-dimensional system of first-order ordinary differential equations is a crucial factor for the manifestation of chaotic behavior, providing a theoretical foundation for the stability observed at these specific points in the host-to-parasite figure.

- Metric 2: Deviation variance on the medium scale:

To evaluate the deviation of the medium time scale F.W. model, we simulate the Inner Iteration process 500 times and calculate the mean of the model deviation variances as follows:

$$\begin{aligned} V_i &= \mathbb{V}(|P_i(t) - \|L_i(t)\|_{L_1}|) . \\ \mathbb{E}(P_i(t)) &= \|L_i(t)\|_{L_1} \end{aligned} \quad (30)$$

where  $\|\bullet\|_{L_1}$  denotes the  $L_1$  norm,  $V_i$  represents the  $i$ -th deviation variance,  $P_i(t)$  and  $L_i(t)$  indicates the  $i$ -th Population number of parasite and the  $i$ -th Male-Female population vector. The latter equation indicates that the mean of the neighbouring two smallest glandular values in the large time scale model equals the integral average of the solution to the medium size model. In the Figure below, we plot the distribution of deviations of the F.W. model.

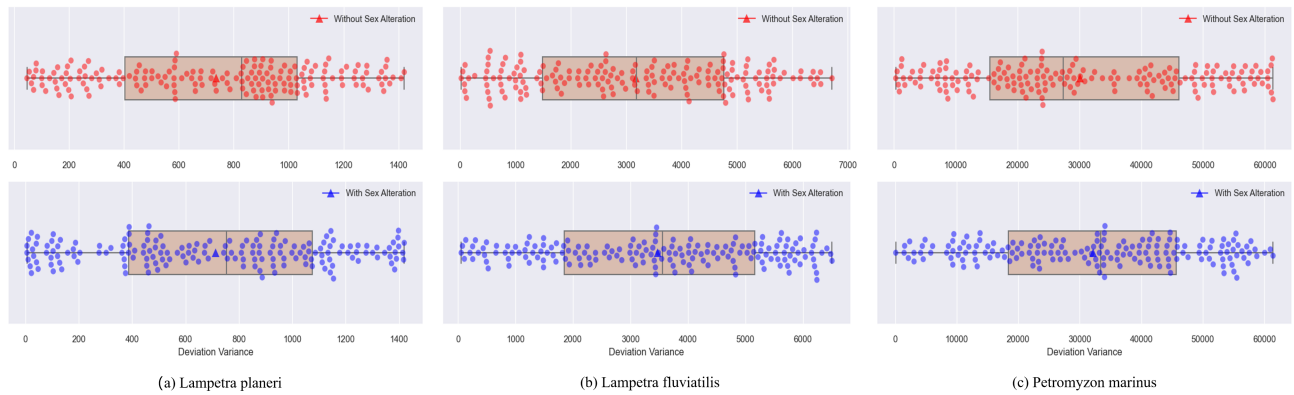


Figure 15: Deviation variance on the medium scale for three species

#### 5.2.4 Impact on the Others in the Ecosystem

In this section, according to the hypothesis, the dominant influencer in the food web of lampreys is the host and its competitors, so we plot the host population as follows:

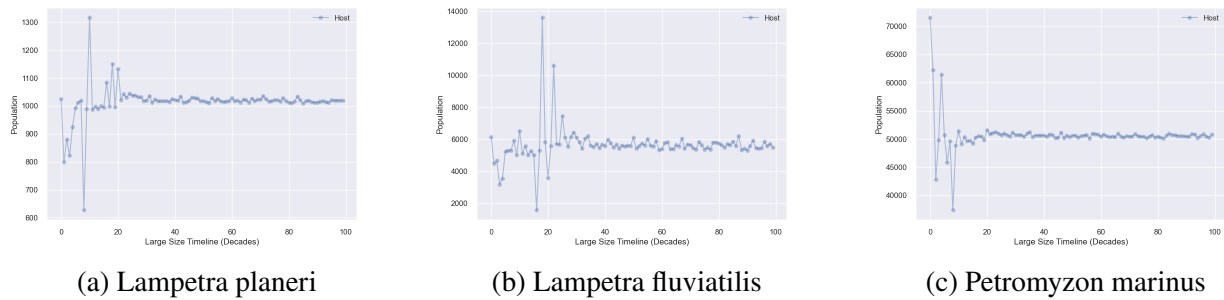


Figure 16: Relations between parasite population and host population

As for the influence on the competitors, Figure 12 demonstrates the interaction among parasites, as mentioned previously, specimen *L.planeri* do not participate in the intense competition of resources, thus enjoying a lower intensity of fluctuation.

## 6 Sensitivity Analysis

As we have analysed the stability of the large time scale model in the previous sections, we focus on the sensitivity analysis of the medium time scale P.D. model.

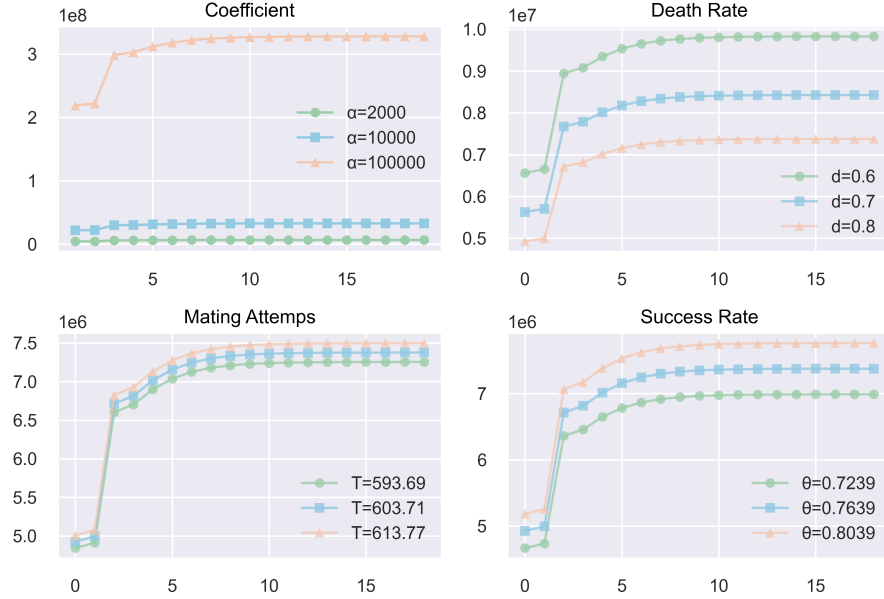


Figure 17: Sensitivity analysis of four variations

In Figure 17, we observe that our model exhibits the highest sensitivity to variations in the survival coefficient, whereas it demonstrates relatively lower sensitivity to changes in the number of mating attempts, verifying that our model is robust to the daily and inter-individual variation of mating activities.

## 7 Further Discussion

### 7.1 Strengths

- We opt for three distinct temporal scales to characterize the characteristics of lampreys. On a large scale, we illustrate trends in the overall quantity and total size  $S_{\text{tot}}$  of lampreys. On a medium scale, we meticulously enumerate the variations in lampreys. Finally, on a small scale, we abstract the fundamental changes during a single mating event, achieving a balanced level of detail and conciseness.
- When we meet the dilemma of a chaotic system in solving the F.W. model, we avoid the reckless computation of the system, but gather a relatively novel numerical approach to approximate the system, and further decouple it with Jacobi Diagonalization, then approximate the derivative vector with the finite difference via the Crank-Nicolson one-step method.
- Utilizing distinctive and comprehensive metrics is essential for gaining nuanced insights during assessment. The evaluation criteria—integrity, measuring ecosystem coherence and robustness, empowerment, exploring ecological vigour, and functionality, scrutinizing operational efficiency—provide unique perspectives, collectively contributing to a thorough analysis of the ecosystem.

## 7.2 Weaknesses

- Modelling, algorithmic, and model errors exist. Modelling errors include defects in the Mating Model, such as size reduction during lamprey mating or sex change. Additionally, the Bayesian model incorporates a limitation on mating occurrences rather than an ideal probability distribution. Algorithmic errors involve a quadratic truncation error in the Crank-Nicolson algorithm. Model deficiencies appear in some biological populations where the granularity of large-scale models is not significantly reduced in medium-scale models.
- The lamprey's role in the food web is examined solely concerning hosts and competitors, neglecting interactions with the broader environment and inorganic components.

## 8 Conclusion

In conclusion, our paper delves into the intricate dynamics of lamprey populations, shedding light on their adaptive responses through sex ratio adjustments. The methodology, structured around the Large Lamprey Model (LLM) comprising the **Population Dynamics (P.D. Model)**, **Mating Model (M. Model)**, and **Food Web Model (F.W. Model)**, spans different time scales, offering a comprehensive perspective on lamprey behaviors.

Strengths of our approach include meticulous model construction, Bayesian integration, and experimental analyses, providing valuable insights. However, recognizing inherent weaknesses, such as modelling errors, algorithmic challenges, and exclusive focus on specific interactions, opens avenues for refinement.

Tasks 1 and 2 reveal potential enhancements in ecological system performance and advantages in challenging environments, tempered by stability concerns. Task 3's extensive P.W. model simulations showcase a stable equilibrium point, and Task 4 elucidates a short-term competitive advantage for lampreys through sex ratio adjustments.

In essence, our paper contributes significant knowledge while setting the stage for future research. Addressing identified weaknesses will refine our understanding of lamprey ecology and advance broader insights into species adaptation and ecological dynamics. The continuous pursuit of scientific excellence promises a deeper comprehension of the intricate relationships between species and their sex ratio strategy.

## 9 References

- [1] Schultz, L. D., Chasco, B. E., Whitlock, S. L., Meeuwig, M. H., Schreck, C. B. (2017). Growth and annual survival estimates to examine the ecology of larval lamprey and the implications of ageing error in fitting models. *Journal of Fish Biology*, 90(4), 1305-1320.
- [2] Daupagne, L., Bouchard, C., Michaud, A., Dhamelincourt, M., Lasne, E., Tentelier, C. (2023). Considering temporal variations in mating opportunities: consequences for sexual selection estimates. *Animal behavior*, 204, 49-65.
- [3] Hunt, J., Breuker, C. J., Sadowski, J. A., Moore, A. J. (2009). Male–male competition, female mate choice and their interaction: determining total sexual selection. *Journal of evolutionary biology*, 22(1), 13-26.
- [4] Hardisty, M.W., Potter, I.C. (1971). The biology of lampreys.
- [5] Smout, S., Asseburg, C., Matthiopoulos, J., Fernández, C., Redpath, S., Thirgood, S., Harwood, J. (2010). The functional response of a generalist predator. *PloS one*, 5(5), e10761.
- [6] Rabajante, J. F., Tubay, J. M., Uehara, T., Morita, S., Ebert, D., Yoshimura, J. (2015). Red Queen dynamics in multi-host and multi-parasite interaction system. *Scientific Reports*, 5(1), 10004.
- [7] Crank, J., Nicolson, P. (1947, January). A practical method for numerical evaluation of solutions of partial differential equations of the heat-conduction type. In *Mathematical proceedings of the Cambridge philosophical society* (Vol. 43, No. 1, pp. 50-67). Cambridge University Press.
- [8] Rall, B. C., Brose, U., Hartvig, M., Kalinkat, G., Schwarzmüller, F., Vucic-Pestic, O., Petchey, O. L. (2012). Universal temperature and body-mass scaling of feeding rates. *Philosophical Transactions of the Royal Society B: Biological Sciences*, 367(1605), 2923-2934.
- [9] Towne, A., Schmidt, O. T., Colonius, T. (2018). Spectral proper orthogonal decomposition and its relationship to dynamic mode decomposition and resolvent analysis. *Journal of Fluid Mechanics*, 847, 821-867.
- [10] May, R. M. (1976). Simple mathematical models with very complicated dynamics. *Nature*, 261(5560), 459-467.
- [11] Johnson, N. S., Buchinger, T. J., Li, W. (2015). Reproductive ecology of lampreys. *Lampreys: Biology, Conservation and Control: Volume 1*, 265-303.
- [12] Uyanik, G. K., Güler, N. (2013). A study on multiple linear regression analysis. *Procedia-Social and Behavioral Sciences*, 106, 234-240.
- [13] Odum, H. T. (2007). Environment, power, and society for the twenty-first century: the hierarchy of energy. Columbia University Press.
- [14] Quintella, B.R., Clemens, B.J., Sutton, T.M., Lança, M.J., Madenjian, C.P., Happel, A., Harvey, C.J. (2021). At-sea feeding ecology of parasitic lampreys. *Journal of Great Lakes Research*.